

Calculating line intensities of 1S_0 emission through standard and modified Judd–Ofelt theories in Pr^{3+} -doped $\text{CaAl}_{12}\text{O}_{19}$ and $\text{SrAl}_{12}\text{O}_{19}$

This article has been downloaded from IOPscience. Please scroll down to see the full text article.

2010 J. Phys.: Condens. Matter 22 155501

(<http://iopscience.iop.org/0953-8984/22/15/155501>)

View [the table of contents for this issue](#), or go to the [journal homepage](#) for more

Download details:

IP Address: 129.252.86.83

The article was downloaded on 30/05/2010 at 07:46

Please note that [terms and conditions apply](#).

Calculating line intensities of 1S_0 emission through standard and modified Judd–Ofelt theories in Pr^{3+} -doped $\text{CaAl}_{12}\text{O}_{19}$ and $\text{SrAl}_{12}\text{O}_{19}$

Jinsu Zhang^{1,2}, Feng Liu³, Xiao-jun Wang^{1,4} and Jiahua Zhang^{1,5}

¹ Key Laboratory of Excited State Processes, Changchun Institute of Optics, Fine Mechanics and Physics, Chinese Academy of Sciences, Changchun 130033, People's Republic of China

² Graduate School of Chinese Academy of Sciences, Beijing 100039, People's Republic of China

³ Department of Physics and Astronomy, University of Georgia, Athens, GA 30602, USA

⁴ Department of Physics, Georgia Southern University, Statesboro, GA 30460, USA

E-mail: zhangjh@ciomp.ac.cn

Received 20 January 2010, in final form 7 March 2010

Published 26 March 2010

Online at stacks.iop.org/JPhysCM/22/155501

Abstract

A modified Judd–Ofelt theory is used in this paper to treat the electric dipole transitions within the $4f^2$ configuration of Pr^{3+} by considering two main perturbing components of $4f5d$ and $4fn'g$. Through the energy-level calculation and standard tensorial analysis, the explicit distance between the $4f5d$ configuration and the 1S_0 state and other lower $4f^2$ energy levels are determined. The rare-earth ion Pr^{3+} substituted at Sr^{2+} sites in $\text{SrAl}_{12}\text{O}_{19}$ (SAO) and Ca^{2+} sites in $\text{CaAl}_{12}\text{O}_{19}$ (CAO) has the site symmetry of D_{3h} . The standard Judd–Ofelt parameters A_{33}^2 , A_{33}^4 , A_{53}^4 , A_{53}^6 , A_{73}^6 are included in the calculation, together with odd- λ parameters A_{33}^3 and A_{53}^5 . The emitting line intensities originating from 1S_0 and 3P_0 are then calculated. Compared with the experimental measurements, the modified model yields better results than the standard Judd–Ofelt theory.

1. Introduction

The standard Judd–Ofelt theory [1, 2] provided a general and successful theoretical framework for calculating the electric dipole transitional intensities between the J multiplets of rare-earth ions. Three parameters Ω_2 , Ω_4 , and Ω_6 were acquired by a fit to the experimental data. In the case of splitting of J induced by the crystal field, Axe [3] studied the transitional intensities between the crystal-field energy levels. Subsequently, a more general parameter set was proposed by Reid and Richardson, A_{tp}^λ [4], which incorporates more information on the structure and on the lanthanide–ligand interaction. The degeneracy of the opposite-parity configurations is assumed in the standard Judd–Ofelt theory. Meanwhile, a closure approximation that the opposite-parity configurations lie far above the $4f^N$ configuration is applied

in the theory. The closure approximation breaks down when applied to the 1S_0 state of trivalent praseodymium, of which the 1S_0 is near the $4f5d$ configuration. To solve the problem, modifications of the standard Judd–Ofelt theory have been introduced [5–8]. Because of the unknown energy-level structure of the opposite-parity configurations, the above modifications are based on the closure approximation. In order to verify the discrepancy of the closure approximation, knowledge of the opposite-parity configurations is desired.

Recently, there has been a growing interest in the study of the high energy spectroscopy of rare-earth ions as part of the effort to design new phosphors for lamps and displays. Dorenbos [9–11] has demonstrated the lowest $4f^{N-1}5d$ state in hundreds of materials. Furthermore, Reid [12] has established a theoretical model to calculate the $4f^{N-1}5d$ energy levels. The development of the above-mentioned has greatly aided the present work.

⁵ Author to whom any correspondence should be addressed.

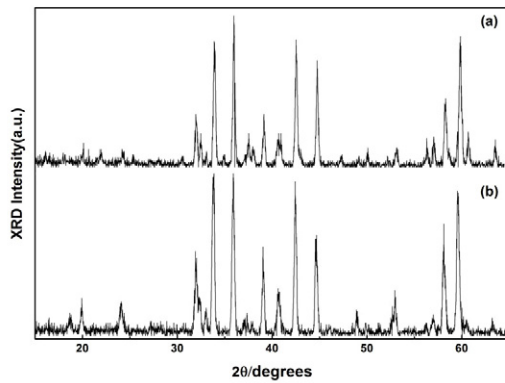


Figure 1. X-ray powder diffraction patterns of (a) $\text{Ca}_{0.99}\text{Al}_{12}\text{O}_{19}:0.01\text{Pr}^{3+}$ and (b) $\text{Sr}_{0.99}\text{Al}_{12}\text{O}_{19}:0.01\text{Pr}^{3+}$.

In this paper, the crystal-field parameters are obtained by fitting the experimental data using f shell programs which are based on the model of Reid. The $4f^2$ and $4f5d$ energy levels of Pr^{3+} are calculated. The opposite-parity mixing states of the $4f5d$ with the $4f^2$ transitional states are determined to give the energy difference between the $4f5d$ and $4f^2$ states. The modified Judd–Ofelt theory is used to calculate the transitional intensities. According to this method, the total transitional intensities from the $^1\text{S}_0$ and $^3\text{P}_0$ levels to the lower J multiplets are calculated by summing over all the transitional intensities between crystal-field levels. Finally, the calculated results by the standard and modified Judd–Ofelt theories are listed and compared with the experimental data. The present method leads to an understanding of the limit of the existing of the standard Judd–Ofelt theory.

2. Experimental details

The single-crystal powder Ce^{3+} and Pr^{3+} doped CAO and SAO samples were prepared by high temperature solid-state reaction. The raw materials CaCO_3 , SrCO_3 , $\gamma\text{-Al}_2\text{O}_3$, and Pr_6O_{11} , CeO_2 with a proper amount of CaF_2 and SrF_2 (5 mol at.%) added as a flux and $\text{Mg}(\text{OH})_2 \cdot 4\text{MgCO}_3 \cdot 6\text{H}_2\text{O}$ acting as a charge compensator were weighed with a definite chemistry dosage. The mixtures were ground homogeneously for 1 h, preheated at 200°C in air for a day, and then sintered at 1500°C in a CO reducing atmosphere for 5 h.

The crystalline structure of the sample was investigated by x-ray diffraction (XRD) patterns with a Cu target radiation source, and a pure SAO or CAO phase was observed, as shown in figure 1. A pure single powder sample was synthesized. The SAO or CAO crystallizes in a face centered cubic structure belonging to the $P6_3/mmc$ space group. The rare-earth dopants occupy Sr^{2+} or Ca^{2+} sites with the point group symmetry of D_{3h} [13]. The photoluminescence excitation (PLE) and diffuse reflection spectra of Ce^{3+} and the photoluminescence (PL) spectrum of $^1\text{S}_0$ to the low lying energy levels of Pr^{3+} were measured using a HITACHI F-4500 fluorescence spectrophotometer. The PL spectrum of $^3\text{P}_0$ to the low lying energy levels of Pr^{3+} was detected by a boxcar-162 integrator upon excitation by an optical parametric oscillator

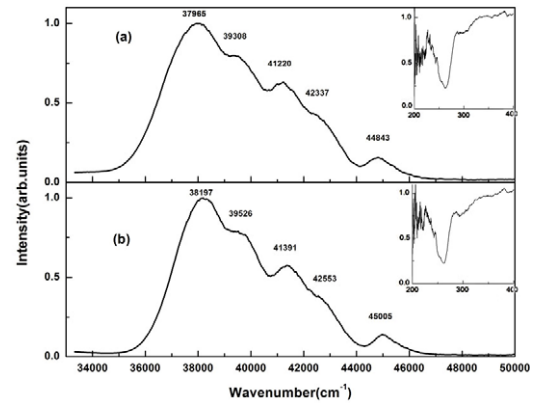


Figure 2. Excitation and diffuse reflection spectra (inside) of (a) $\text{Ca}_{0.99}\text{Al}_{12}\text{O}_{19}:0.01\text{Ce}^{3+}$ and (b) $\text{Sr}_{0.99}\text{Al}_{12}\text{O}_{19}:0.01\text{Ce}^{3+}$ monitored at 324 nm and 307 nm, respectively.

(OPO). All of the spectra have been corrected by the response of the detector. The fluorescence lifetime of $^3\text{P}_0$ was detected at a low temperature of 10 K.

3. Result and discussion

3.1. Energy-level calculation

The energy levels of the $4f^2$ and $4f5d$ configurations are calculated by f shell programs. The free ions and crystal-field parameters for the $4f^2$ configuration are taken from [14] and [15], respectively. The crystal-field parameters for 5d electrons are obtained by fitting the excitation spectra of Ce^{3+} -doped CAO and SAO shown in figure 2. In this paper, we adopt antitheses to analyze the factors which affect the position of the $4f5d$ configuration of Pr^{3+} according the spectra of Ce^{3+} . The barycenter of the $4f5d$ configuration lies in the vacuum ultraviolet region, which will fall with increasing covalence. The splitting range of the $4f5d$ configuration depends on the crystal-field strength. Figure 2 shows the excitation and diffuse reflection spectra of the Ce^{3+} doped CAO and SAO systems. The diffuse reflection spectra of Ce^{3+} exhibits the lowest 5d configuration located at 37965 cm^{-1} in CAO and 38197 cm^{-1} in SAO, indicating an energy difference of about 232 cm^{-1} . The onset absorption of the Pr^{3+} $4f5d$ bands is at 212 nm (47170 cm^{-1}) and 211 nm (47393 cm^{-1}) in CAO and SAO, respectively [16]. The covalence of alkaline earth metal ion Ca^{2+} is stronger than Sr^{2+} , so the barycenter of the 5d configuration of Ce^{3+} in CAO is lower than that in SAO. Otherwise, the cation–anion distance in CAO (average Ca–O distance approximate 2.71 \AA) [17] is shorter than that in SAO (average Sr–O distance approximate 2.83 \AA) [18], enhancing the crystal-field strength in the CAO host. In other words, the 5d configuration splitting of Ce^{3+} in CAO is larger than that in SAO. From the excitation spectrum of Ce^{3+} , we find that the splitting range of the 5d configuration is about 6878 cm^{-1} in CAO and 6808 cm^{-1} in SAO. The energy difference is only 70 cm^{-1} , which is much smaller than 232 cm^{-1} , the energy difference of the lowest 5d configuration. We can conclude from the above analysis that the barycenter shift will

have a relative large contribution to the position of the 5d configuration in Ce³⁺-doped CAO and SAO systems. Finally, the 5d crystal-field parameters B_{kq} (dd) are obtained by fitting the excitation spectra of Ce³⁺ which give the 5d energy levels of Ce³⁺. The difference of the f-d barycenter Δ_E (fd) is adjusted. Agreement between the experimental and calculation results has been achieved. Next, we obtain the values of the parameters: Δ_E (fd) = 39 493 cm⁻¹, 39 593 cm⁻¹ and B_{20} (dd) = 759 cm⁻¹, 748 cm⁻¹ and B_{40} (dd) = 11 187 cm⁻¹, 11 057 cm⁻¹ for Ce³⁺ in CAO and SAO. The fitting results show a good agreement with the above analysis, furthermore the 4f5d energy levels of Pr³⁺ are calculated.

3.2. Calculation method and f-f intensity parameters

In rare-earth doped system, the intraconfigurational f-f electric dipole transitions can arise from the admixture of the 4f^N transitional states with their opposite-parity configurations. These perturbing configurations have a higher energy than the 4f^N configurations and are mostly of the type 4fn'd and 4fn'g [1]. The perturbing configuration of 4f5d for the type 4fn'd is considered. The configurations for $n' \geq 6$ of the type 4fn'd can be neglected due to the much smaller quantity in the intensity calculation. All the configurations of the type 4fn'g should be considered for the admixture. The nonzero matrix elements of the electric dipole operator between the initial $\langle \varphi_i |$ and final states $|\varphi_f\rangle$ of the 4f^N are

$$\langle 4f^N \varphi_i | \hat{D}_p^1 | 4f^N \varphi_f \rangle = \sum_{\varphi''} \left[\frac{\langle \varphi_i | \hat{D}_p^1 | \varphi_i'' \rangle \langle \varphi_i'' | H_{CF} | \varphi_f \rangle}{E(\varphi_f) - E(\varphi_i'')} + \frac{\langle \varphi_f | \hat{D}_p^1 | \varphi_f'' \rangle \langle \varphi_f'' | H_{CF} | \varphi_i \rangle}{E(\varphi_i) - E(\varphi_f'')} \right] \quad (1)$$

where the corresponding Hamiltonian can be written as

$$H_{CF}(\text{odd}) = \sum_{k,q,j} A_q^k \cdot r^k \hat{c}_q^k(j), \quad k = \text{odd number.} \quad (2)$$

The electric dipole operator \hat{D}_p^1 , which dominates the relevant transition, is then expressed as

$$\hat{D}_p^1 = \sum_j r \hat{c}_p^1(j). \quad (3)$$

In equation (1) the subscript i and f denote the initial or final mixing states, and \hat{c}_q^k is the irreducible tensor operator of rank k ; the values of q are determined by site symmetry.

In this paper, we will focus on the two major transitions originating from the ³P₀ and ¹S₀ initial states of Pr³⁺. Two major opposite-parity configurations of 4f5d and 4fn'g have been considered in the admixture. The Judd-Ofelt theory gives an expression for the electric dipole transitional strengths between the initial state and final state

$$\langle i | D_p^{(1)} | f \rangle_g = \sum_{k,q,\lambda} A_{kq(g)}^\lambda [k]^{1/2} (-1)^{p+q+J-M} \times \begin{pmatrix} 1 & \lambda & k \\ p & -p-q & q \end{pmatrix} \begin{pmatrix} J & \lambda & J' \\ -M & p+q & M' \end{pmatrix} \times \langle \varphi J || U^{(\lambda)} || \varphi' J' \rangle \quad (4)$$

where

$$A_{kq(g)}^\lambda = -A_{kq} \Xi(k, \lambda)_{(g)} (2\lambda + 1) / \sqrt{2k + 1} \\ \Xi(k, \lambda)_{(g)} = 14 \sum_{n'g} (2 \times 4 + 1) (-1)^{4+3} \\ \times \begin{Bmatrix} 1 & \lambda & k \\ 3 & 4 & 3 \end{Bmatrix} \begin{pmatrix} 3 & 1 & 4 \\ 0 & 0 & 0 \end{pmatrix} \begin{pmatrix} 4 & k & 3 \\ 0 & 0 & 0 \end{pmatrix} \frac{\langle r \rangle \langle r^k \rangle}{\Delta(n'g)}.$$

$\langle r \rangle$ and $\langle r^k \rangle$ in the above equation are the radial integrals between different configurations. The approximation $\sum_{n'} \langle 4f | \hat{r} | n'g \rangle \langle 4f | \hat{r}^k | n'g \rangle = \langle 4f | \hat{r}^{k+1} | 4f \rangle$ can be applied to the 4fn'g configuration [19]. The energy denominator of the initial state $E(\varphi_i) - E(\varphi_i'')$ and the final state $E(\varphi_f) - E(\varphi_f'')$ are assumed equal, in other words it is assumed that the perturbing configurations lie far above the optical transitional states within the 4f shell. This assumption is suitable for the 4fn'g configuration due to the large energy difference from the 4f² configuration. Nevertheless, the 4f5d configuration is near above the 4f² transitional states, especially for the ¹S₀ state, the energy levels of 4f² and 4f5d are calculated, and the main 4f5d components mixed into the 4f² initial and final states will be determined.

The f-d mixing is determined by calculating the matrix elements of the irreducible tensor operator about the electric dipole transitions $\langle \varphi_i | \hat{D}_p^1 | \varphi_i'' \rangle$ and $\langle \varphi_f | \hat{D}_p^1 | \varphi_f'' \rangle$ and odd-rank crystal fields $\langle \varphi_i'' | H_{CF} | \varphi_f \rangle$ and $\langle \varphi_f'' | H_{CF} | \varphi_i \rangle$ between the states of 4f² and 4f5d. In Pr³⁺ doped SAO, a detailed analysis is reported in [20] to give the opposite-parity mixing states with the ³P₀ and ¹S₀ initial or final transition states in D_{3h} symmetry, which will be used to confirm the values of the energy denominators $E(\varphi_f) - E(\varphi_f'')$ and $E(\varphi_i) - E(\varphi_i'')$ in our calculation. An analogous calculation will be done in the Pr³⁺ doped CAO, and the corresponding opposite-parity mixing states and their values are listed in table 1.

The ¹S₀ of Pr³⁺ lies so near the 4f5d configuration that discrepancies are observed when the Judd-Ofelt theory is applied to treat the intensity calculation for the ¹S₀ state. Here, we consider the difference of energy denominators in the initial and final transitional states and give a modified expression

$$\langle i | \hat{D}_p^{(1)} | f \rangle_d = \sum_{k,q,\lambda} A_{kq(d)}^\lambda [k]^{1/2} (-1)^{p+q+J-M} \\ \times \left(\frac{1}{E(\varphi_f) - E(\varphi_f'')} + \frac{(-1)^{1+\lambda+k}}{E(\varphi_i) - E(\varphi_i'')} \right) \\ \times \begin{pmatrix} 1 & \lambda & k \\ p & -p-q & q \end{pmatrix} \begin{pmatrix} J & \lambda & J' \\ -M & p+q & M' \end{pmatrix} \\ \times \langle \varphi J || U^{(\lambda)} || \varphi' J' \rangle \quad (5)$$

where

$$A_{kq(d)}^\lambda = -A_{kq} \Xi(k, \lambda)_{(d)} (2\lambda + 1) / \sqrt{2k + 1} \\ \Xi(k, \lambda)_{(d)} = 7 \sum_{5d} (2 \times 2 + 1) (-1)^{2+3} \\ \times \begin{Bmatrix} 1 & \lambda & k \\ 3 & 2 & 3 \end{Bmatrix} \begin{pmatrix} 3 & 1 & 2 \\ 0 & 0 & 0 \end{pmatrix} \begin{pmatrix} 2 & k & 3 \\ 0 & 0 & 0 \end{pmatrix} \langle r \rangle \langle r^k \rangle.$$

The reduced matrix element $\langle \varphi J || U^{(\lambda)} || \varphi' J' \rangle$ can be calculated using the doubly reduced matrix elements $\langle f^N \gamma S L || U^{(\lambda)} || f^N \gamma' S' L' \rangle$ which are tabulated by Nielson and Koster [21]. The

Table 1. The opposite-parity mixing states of the 4f5d with 1S_0 and 3P_0 states in Pr^{3+} doped CAO and SAO and their energy values.

4f2 configuration Initial states 4f2SLJM	4f5d configuration					
	Mixing with initial states 4f5dS''L''J''M''	Energy denominators		Mixing with final states 4f5dS''L''J''M''	Energy denominators	
		CAO	SAO		CAO	SAO
$^1S_{0(0)}$	$^1F_{3(-3,+3)}$	64 062	63 934	$^3P_{1(\pm 1)}$	61 687	61 660
	$^1H_{5(-3,+3)}$	72 244	72 221	$^1P_{1(0)}$	72 556	72 518
$^3P_{0(0)}$	$^3D_{3(-3,+3)}$	62 615	62 585	$^3D_{1(\pm 1)}$	61 663	61 629
	$^3G_{3(-3,+3)}$	58 520	58 103	$^3D_{1(0)}$	61 801	61 779
	$^3G_{5(-3,+3)}$	63 145	63 100			

matrix element includes both even and odd terms. $\Xi(k, \lambda)_{(g)}$ in equation (4) contains the information about the average difference between the 4f² and 4fn'g configurations. $\Xi(k, \lambda)_{(g)}$ is considered as an unknown quantity in standard Judd–Ofelt theory, while in the calculation for dealing with the mixing of the 4f5d configuration, the energy denominators are known quantitatively and appear in the transitional expression. The (\dots) and $\{\dots\}$ in equations are the $3 - j$ and $6 - j$ symbols, respectively, and $[k]$ equals to $2k + 1$. The Judd–Ofelt theory considers the same energy denominators, so the nonzero condition of equation (4) requires even- λ because the exponent $1 + \lambda + k$ should be even and k is odd in equation (2), whereas both even and odd λ are included in equation (5) because of the difference of the energy denominators.

The electric dipole and strengths between an initial state φJ and a final state $\varphi' J'$ in Judd–Ofelt theory is written as

$$S^{\text{ED}}(\varphi J, \varphi' J') = e^2 \sum_{i,f} |\langle i | \hat{D}_p^{(1)} | f \rangle_g + \langle i | \hat{D}_p^{(1)} | f \rangle_d|^2. \quad (6)$$

The radiative decay rates for electric dipole transitions is expressed as

$$A(\varphi J, \varphi' J') = \frac{64\pi^4 \sigma^3}{3h(2J + 1)} \chi^{\text{ED}} S^{\text{ED}}(\varphi J, \varphi' J'), \quad (7)$$

where $\chi^{\text{ED}} = \frac{n(n^2+2)^2}{9}$ is the Lorentz local field correction factor for the electric dipole emission. We have approximated the index versus wavelength in SAO and CAO by $n_{(\lambda)} = 1.75 + (12700 \text{ nm}^2)/\lambda^2$, obtained according to the closely related crystal $\text{LaMgAl}_{11}\text{O}_{19}$ [22], because all three of them have almost the same hexagonal magnetoplumbite structure. e is the elementary charge; h is Planck's constant; and σ is the wavenumber at the emission maximum.

In the present D_{3h} site symmetry, the necessary phenomenological intensity parameters are determined by equations (4) and (5) and a set of intensity parameters $A_{33(g)}^2$, $A_{33(g)}^4$, $A_{53(g)}^4$, $A_{53(g)}^6$ and $A_{73(g)}^6$, together with $A_{33(d)}^2$, $A_{33(d)}^4$, $A_{53(d)}^4$, $A_{53(d)}^6$ and $A_{73(d)}^6$, are included. The relationships between these parameters are calculated using equations (4) and (5):

$$\begin{aligned} \frac{A_{33(d)}^3}{A_{33(d)}^2} &= -2.4749 & \frac{A_{33(d)}^4}{A_{33(d)}^2} &= 3.5178 \\ \frac{A_{53(d)}^5}{A_{53(d)}^4} &= -3.6667 & \frac{A_{53(d)}^6}{A_{53(d)}^4} &= 9.6896 \end{aligned}$$

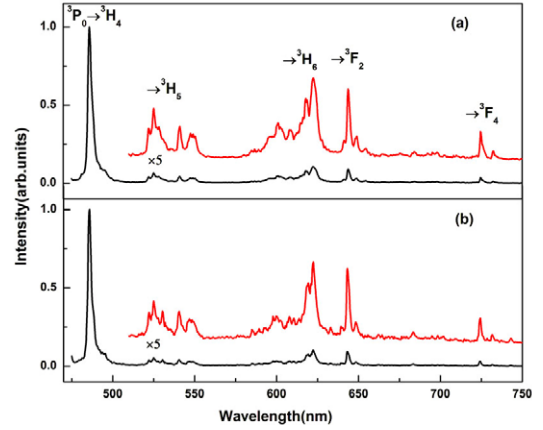


Figure 3. Emission spectra of (a) $\text{Ca}_{0.99}\text{Al}_{12}\text{O}_{19}:0.01\text{Pr}^{3+}$ and (b) $\text{Sr}_{0.99}\text{Al}_{12}\text{O}_{19}:0.01\text{Pr}^{3+}$ upon $^3H_4 \rightarrow ^1P_0$ excitation (466 nm). (This figure is in colour only in the electronic version)

$$\frac{A_{33(g)}^4}{A_{33(g)}^2} = 0.3838 \quad \frac{A_{53(g)}^6}{A_{53(g)}^4} = 0.1242.$$

Thus, only five parameters $A_{33(d)}^2$, $A_{53(d)}^4$, $A_{33(g)}^4$, $A_{53(g)}^4$ and $A_{73(g)}^6$ in the intensity calculation perform an important function. The intensity parameters A_{kq}^{λ} contain the unknown quantities of the odd-rank crystal-field coefficients A_{kq} and the interconfigurational radial integral $\langle r \rangle$ and $\langle r^k \rangle$. Their values are usually calculated according to the Hartree–Fock method [23, 24]. In this work, the initial values of intensity parameters are determined according to the values of A_{kq} in [1] and the values of $\langle r \rangle$ and $\langle r^k \rangle$ in [25]. The final given values are obtained by fitting the measured data through the least-squares deviation [26].

3.3. Intensity calculation and comparison with Judd–Ofelt theory

In the Pr^{3+} doped SAO and CAO system, the intensity parameters $A_{33(d)}^2$, $A_{53(d)}^4$, $A_{33(g)}^4$, $A_{53(g)}^4$ and $A_{73(g)}^6$ are determined by fitting the relative transitional intensities originating from the 3P_0 level to the lower lying SLJ multiplets. The experimental data are shown in table 2, which are obtained by integrating the emission spectrum shown in figure 3. The calculated intensity ratios for the transition to the SLJ states are obtained through summing over all the electric dipole

Table 2. Experimental and calculated transition strengths from 3P_0 in Pr^{3+} -doped CAO and SAO.

Final states [$f^N[SL]J$]	Energy difference (cm^{-1})	CAO			SAO		
		This work	Judd–Ofelt	Measured	This work	Judd–Ofelt ^a	Measured ^a
3H_4	20 654	1.000	1.000	1.000	1.000	1.000	1.000
3H_5	18 568	0.004	0.000	0.082	0.004	0.000	0.086
3H_6	16 396	0.072	0.432	0.204	0.085	0.457	0.183
3F_2	15 759	0.119	0.000	0.121	0.119	0.000	0.117
3F_4	13 935	0.246	0.213	0.065	0.246	0.213	0.063
Lifetime		30 μs	30 μs	30 μs [25]	36 μs	36 μs	36 μs [10]

^a Taken from the data in [10].**Table 3.** Experimental and calculated transition strengths from 1S_0 in Pr^{3+} -doped CAO and SAO.

Final states [$f^N[SL]J$]	Energy difference (cm^{-1})	CAO			SAO		
		This work	Judd–Ofelt	Measured	This work	Judd–Ofelt ^a	Measured ^a
3H_4	46 699	0.126	0.049	0.195	0.126	0.049	0.125
3F_4	39 981	0.68	0.326	0.519	0.680	0.326	0.549
1G_4	36 967	1.000	1.000	1.000	1.000	1.000	1.000
1D_2	29 886	0.102	0.000	0.089	0.101	0.000	0.067
1I_6	25 400	0.196	0.857	0.484	0.231	0.907	0.344
Lifetime		482 ns	2160 ns	650 ns [25]	569 ns	2600 ns	678 ns [10]

^a Taken from the data in [10].

intensities between crystal-field levels with the SLJ multiplets. The ratio of the intensity parameters will be determined by a least-square fitting between the measured and calculated data. Furthermore, in order to determine the absolute magnitude of the fitted variants, the natural lifetime of 3P_0 is needed. In the condition of low Pr^{3+} concentrations and low temperatures, the cross-relaxation and nonradiative processes of 3P_0 can be ignored, thus the measured lifetime is considered as the inverse of all the probabilities of the radiative transitions in equation (7). Then the intensity parameters are listed as follows:

$$A_{33(d)}^2 = -30.67 \times 10^{-7}, \quad A_{53(d)}^4 = 7.43 \times 10^{-7},$$

$$A_{33(g)}^2 = -0.0063 \times 10^{-12} \text{ cm}, \quad A_{53(g)}^4 = 0.0071 \times 10^{-12} \text{ cm}$$

and $A_{73(g)}^6 = -0.1104 \times 10^{-12} \text{ cm}$

for Pr^{3+} in CAO

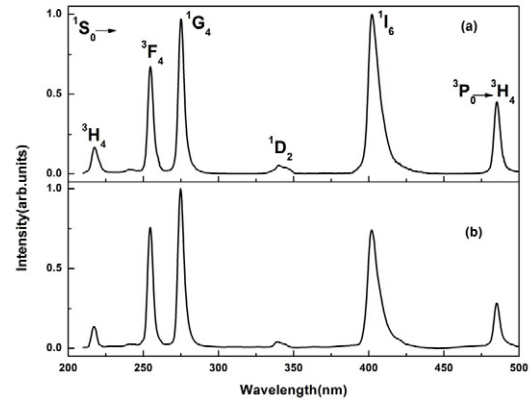
$$A_{33(d)}^2 = -27.90 \times 10^{-7}, \quad A_{53(d)}^4 = 6.85 \times 10^{-7},$$

$$A_{33(g)}^2 = -0.0057 \times 10^{-12} \text{ cm}, \quad A_{53(g)}^4 = 0.00645 \times 10^{-12} \text{ cm}$$

and $A_{73(g)}^6 = -0.1040 \times 10^{-12} \text{ cm}$

for Pr^{3+} in SAO.

The given intensity parameters have a good interpretation for the 3P_0 emission spectra. The calculated data from the present work and those from the standard Judd–Ofelt treatments, along with the experimental data are all listed in table 2. It can be noted that the hypersensitive transition of $^3P_0 \rightarrow ^3F_2$ has been described well with experimental measurements. It is also worth noting that the transition of $^3P_0 \rightarrow ^3H_5$ is forbidden in the standard Judd–Ofelt theory, but it is allowed in the present work. By comparing the data listed in table 2, we can see that the present calculated method shows a good agreement with the measurements.

**Figure 4.** Emission spectra of (a) $Ca_{0.99}Al_{12}O_{19}:0.01Pr^{3+}$ and (b) $Sr_{0.99}Al_{12}O_{19}:0.01Pr^{3+}$ upon $^3H_4 \rightarrow ^1S_0$ excitation (198 nm).

The emitting intensities originating from higher energy level 1S_0 are obtained, as listed in table 3. The experimental data are obtained by integrating the emission spectrum shown in figure 4. Due to the proximity of the $4f5d$ configuration, the modified model yields better results than the standard Judd–Ofelt theory. In order to make this more obvious further work will be done. A computer program for the theoretical spectrum will be completed.

4. Conclusions

The crystal-field parameters for $5d$ electrons in CAO and SAO single powders are fitted to the Ce^{3+} spectra. Next, the accurate energy-level schematics of the $4f^2$ and $4f5d$ configurations in Pr^{3+} doped CAO and SAO systems are calculated. Furthermore, a theoretical method for calculating the electric dipole transitional intensities within the $4f^2$

configuration in Pr³⁺ doped CAO and SAO systems has been proposed. Two major opposite-parity configurations of 4f5d and 4fn'g have been considered for the parity-state mixing. The explicit mixing 4f5d compositions have been given. The values of intensity parameters are determined by the least-squares fitting between the experimental and calculated data. The present calculated method gives better results than the standard Judd–Ofelt treatments for the optical transition of the ¹S₀ and ³P₀ energy levels.

Acknowledgments

This work is financially supported by the National Nature Science Foundation of China (10834006, 10774141, 10904141, 10904140), the MOST of China (2006CB601104), the Scientific project of Jilin province (20090134, 20090524) and the CAS Innovation Program.

References

- [1] Judd B R 1962 *Phys. Rev.* **127** 750
- [2] Ofelt G S 1962 *J. Chem. Phys.* **37** 511
- [3] Axe J D 1963 *J. Chem. Phys.* **39** 1154
- [4] Reid M F and Richardson F S 1983 *J. Chem. Phys.* **79** 5735
- [5] Levey C G 1990 *J. Lumin.* **45** 168
- [6] Quimby R S and Miniscalco W J 1994 *J. Appl. Phys.* **75** 613
- [7] Merkle L D, Zandi B, Moncorge R, Guyot Y, Verdun H R and McIntosh B 1996 *J. Appl. Phys.* **79** 1849
- [8] Goldner P and Auzel F 1996 *J. Appl. Phys.* **79** 7972
- [9] Dorenbos P 2000 *J. Lumin.* **91** 91
- [10] Dorenbos P 2000 *Phys. Rev. B* **62** 15640
- [11] Dorenbos P 2000 *Phys. Rev. B* **62** 15650
- [12] Reid M F, van Pieterse L, Wegh R T and Meijerink A 2000 *Phys. Rev. B* **62** 14744
- [13] Merkle L D, Zandi B, Moncorge R, Guyot Y, Verdun H R and McIntosh B 1996 *J. Appl. Phys.* **79** 1849
- [14] van Pieterse L, Reid M F, Wegh R T, Sovarna S and Meijerink A 2002 *Phys. Rev. B* **65** 045113
- [15] Zandi B, Merkle L D, Gruber J B, Wortman D E and Morrison C A 1997 *J. Appl. Phys.* **81** 1047
- [16] Nie Z, Zhang J, Zhang X, Ren X, Di W, Zhang G, Zhang D and Wang X-J 2007 *J. Phys.: Condens. Matter* **19** 076204
- [17] Utsunomiya A, Tanaka K, Morikawa H and Marumo F 1988 *J. Solid State Chem.* **75** 197
- [18] Kimura K, Ohgaki M, Tanaka K, Morikawa H and Marumo F 1990 *J. Solid State Chem.* **87** 186
- [19] Görrler-Walrand C and Binnemans K 1998 *Handbook on the Physics and Chemistry of Rare Earths* vol 25, ed K A Gschneidner Jr and L Eyring (Amsterdam: North-Holland) p 140
- [20] Liu F, Zhang J, Lu S, Liu S, Huang S and Wang X-J 2006 *Phys. Rev. B* **74** 115112
- [21] Nielson C W and Koster G F 1963 *Spectroscopic Coefficients for the pⁿ, dⁿ, and fⁿ Configurations* (Cambridge: MIT Press)
- [22] Bykovskii P I, Lebedev V A, Pisarenko V F and Popov V V 1986 *J. Appl. Spectrosc.* **44** 425
- [23] Morrison C A and Leavitt R P 1979 *J. Chem. Phys.* **71** 2366
- [24] Esterowitz L, Bartoli F J, Allen R E, Wortman D E, Morrison C A and Leavitt R P 1979 *Phys. Rev. B* **19** 6442
- [25] Reid M F, van Pieterse L and Meijerink A 2002 *J. Alloys Compounds* **344** 240
- [26] Porcher P and Caro P 1978 *J. Chem. Phys.* **68** 4176